Proceedings of the
International Conference on Mechanical Engineering and Renewable Energy 2019
(ICMERE2019) 11 – 13 December, 2019, Chittagong, Bangladesh

ICMERE2019-PI-063

INVESTIGATION OF STRUCTURAL AND MORPHOLOGICAL PROPERTIES OF DISTORTED MONOCLINIC HEMATITE NANOPARTICLES

Md. Khairul Islam, Md. Rahat Al Hassan, Aungkan Sen

Dept. of Glass & Ceramic Engineering (GCE), Rajshahi University of Engineering & Technology (RUET),Rajshahi-6204, Bangladesh.

E-mail: ikhairul277@gmail.com, rahatmme9@gmail.com, senaungken@gmail.com

Abstract*-The diverse properties of hematite nanoparticles are strongly co-related to its structure, size and synthesis technique. In this study, hematite (α-Fe_2O_3) nanoparticles were obtained through facile sol-gel synthesis route utilizing Ferric Nitrate nonahydrate as precursor material. The synthesized nanopowders were annealed at three different temperatures: 400^o C, 600^o C and 800^o C respectively. Effects of annealing temperature variation on crystallinity of hematite were observed from XRD patterns. Moreover, monoclinic hematite phase (space group P 1 21 1) presence was confirmed by Reitveld refinement. The particle size was found around 40 nm and increased with rising annealing temperature. Higher annealing temperature leads to the formation of finer and nearly spherical shaped hematite nanoparticles which was revealed by SEM pictures. The optical properties of hematite powders were studied by applying UV-Visible spectroscopic technique.*

Keywords: Hematite nanoparticles, Sol-gel technique, Monoclinic, XRD, SEM.

1. Introduction

Hematite (α-Fe_2O_3) nanoparticles, a polymorph of Iron oxide, has been drawn substantial attention now a days because of its unique physical and chemical properties as a result of their small size which leads to the presence of large no. of atoms on the surface enabling high surface energy [4]. This effect influences the surface morphologies to control the nanostructure. Being smaller in size, lower sintering temperature and time is required for hemamtite nanoparticles thus involving reduced energy cost. Different fabrication routes strongly controls the structural morphology: size, shape and composition of hematite nanopowder. It is possible to obtain various crystal structure such as rhombohedral, monoclinic or hexagonal by closely controlling the applied synthesis parameters [12]. Several chemical tecniques such as ball millig, chemical vapor deposition, coprecipitation, sol-gel process, hydrothermal synthesis, micro-emulsion techniques, pyrolysis have been employed for the preparation of hematite nanoparticles [1-4,7]. Despite of all these techniques, synthesis of hematite with highly dispersion and uniform size distribution is still a challenge [3, 6]. But sol-gel method is more suitable than others because handling of chemicals is easy and it gives more control of size and shape of the fabricated powder [5].

The most notable properties of hematite is high corrosion resistance which accounts for its application in photo anode [2]. This is because of its band gap lies within the range 2.0 – 2.2, therefore helps absorbing a large fraction of solar spectrum and chemical stability. It is an active agents for gas sensing application and used as a catalyst. It is also used in ferrofluids, medicine, pigment and coating application [3, 7].

In this study, nanosized hematite particles has been fabricated by sol-gel processing route. Deformation in the crystal structure and surface morphology has been thoroughly studied using XRD together with Rielveld refinement and SEM analysis. The optical absorption and band gap are determined using UV visible spectroscopy.

2. Experimental Details

Hematite nanoparticles were fabricated by a facile sol-gel method employing Ferric nitrate nonahydrate as starting material and citric acid as gelating media. At first 5 gm ferric nitrate and 4 gm citric acid were dissolved in 100 ml ethanol

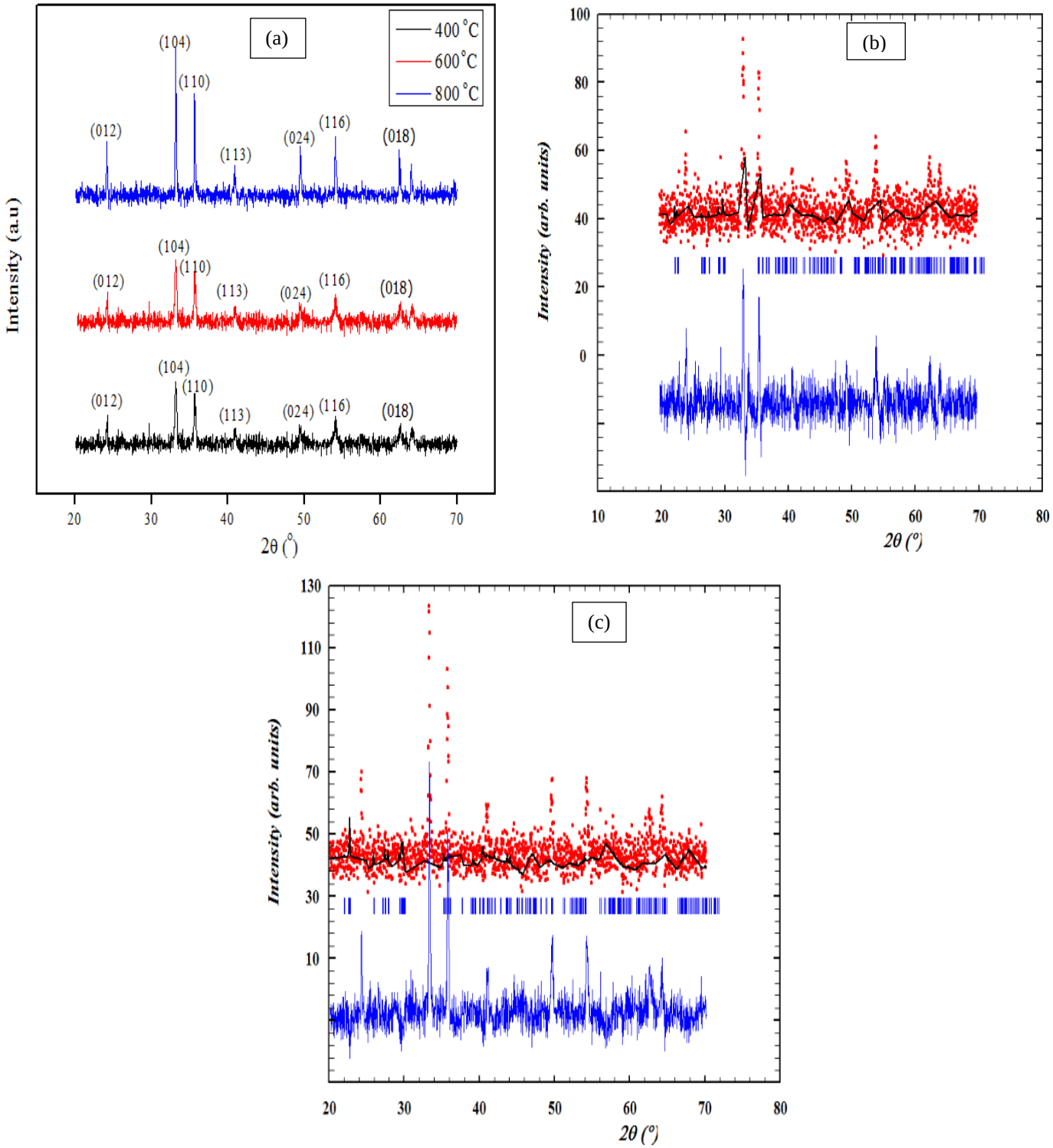

Fig.1: (a) XRD patterns of Hematite (α-Fe_2O_3) nanoparticles; (b) Rietveld refinement of samples annealed at 400° C and (c) 600° C.

solution and magnetically stirred for 50 min at 60 °C for fully dissolution while keeping the P^H value close to 2.0. The resulting gel was dried at 80 °C for 6 hours using a hot plate. After that the obtained red compound was left in oven for overnight drying at 110 °C. Grinding of the sample into powder form was next followed by employing mortar-pestle arrangement. The produced powder was annealed at three different temperature: 400°, 600° and 800° C respectively in a muffle furnace.

X-ray diffraction pattern was employed to find out the crystalline morphology and to get a clear concept about crystallite size using Brukers-D8 Advanced diffractometer

Table 1: Structural parameters of hematite samples

Composition	Space group	Cell Parameter (Å)	Volume ($Å^3$)	R factors (%)	GoF	Bragg R Factor
Hematite-400	P 1 21 1	a = 4.80	252.51	11.6	1.1	93.9
		b = 8.06				
		c = 6.91				
Hematite-600	P 1 21 1	a = 4.75	251.68	10.4	0.95	94.5
		b = 8.07				
		c = 6.93				
Hematite-800	P 1 21 1	a = 4.82	255.68	10.7	0.85	99.8
		b = 8.08				
		c = 6.94				

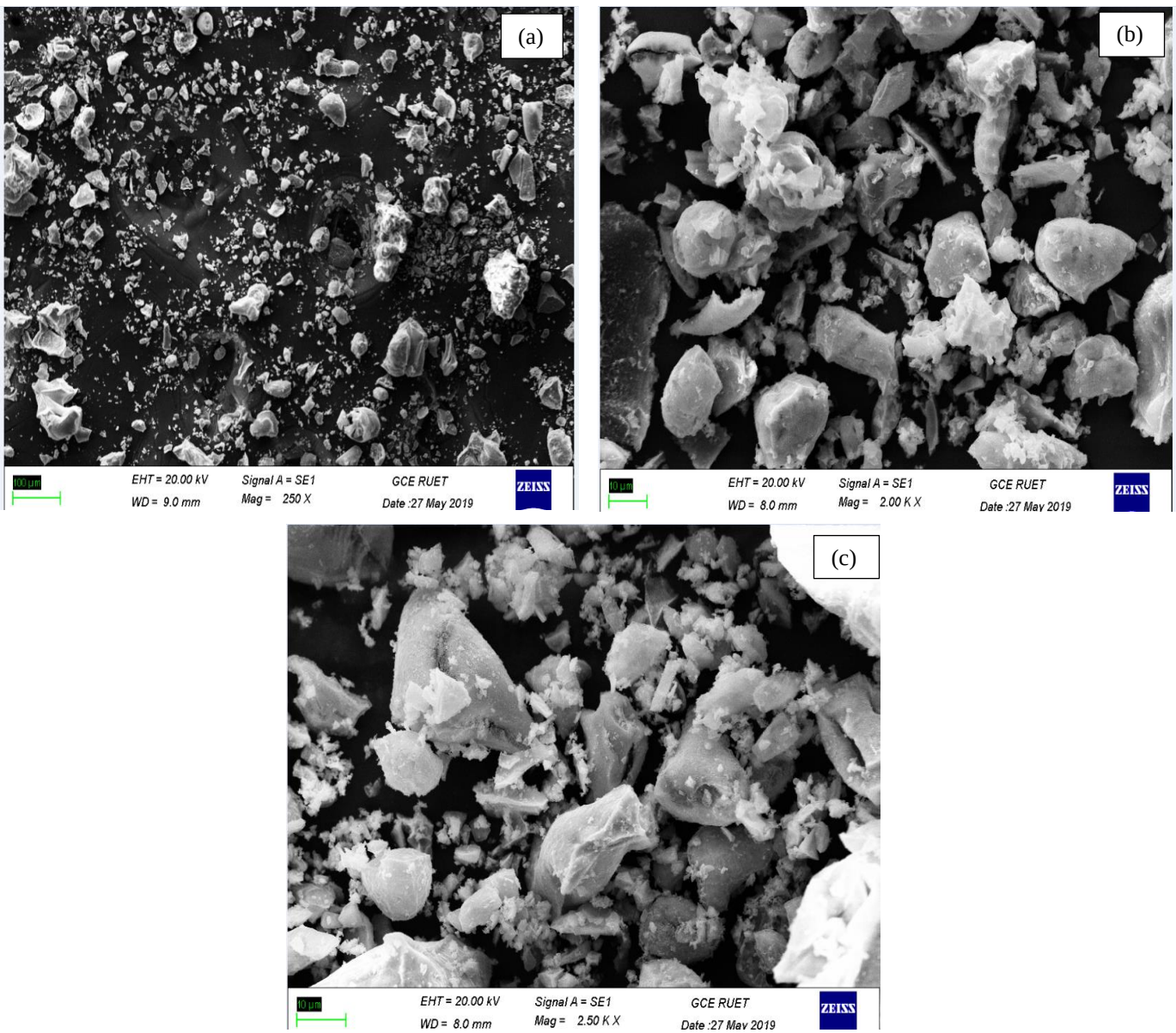

Fig.2: SEM micrographs of hematite samples annealed at (a) 400^o (b) 600^o and (c) 800^o C

Table 2: Average grain size and Optical band energy of hematite samples

Samples	Annealing temperature (^{o} C)	Grain size, d (μm)	Band Gap, E_g (eV)
Hemataite-1	400	16.3	4.90
Hemataite-2	600	40.2	4.95
Hemataite-3	800	47.1	4.80

with Cu Kα radiation with 2θ in the range 20^o-70^o. Rietveld refinement was carried out using FULLPROF software. Surface properties were analyzed by SEM (ZEISS-EVO 18). UV-Visible spectroscopy (SHIMADJU UV-Vis PC 1650) was utilized to confirm the absorption spectra and calculate the band gap. To completely disperse, hematite powders were dissipated in ethanol and vibrated using an Ultrasonic bath before the measurement.

3. Results and Discussion

3.1 XRD

The XRD patterns of hematite nanoparticles annealed at 400^o, 600^o and 800 ^{o}C respectively are shown in Fig. 1. The diffraction spectra and Rietveld analysis revealed the formation of monoclinic crystalline form of hematite instead of rhombohedral with no impurity phase for all three samples which is in line with previous research (JCPDS card no. 33-0664). The space group was found same for all samples: P-1 21 1. Lattice parameter and other structural values are displayed in Table 1.

The high intensity peaks at (012), (104), (110), (113), (024), (116) and (018) indicated the complete homogeneous liquid phase reaction [8, 9]. The characteristic peak (104) increases with rising anealling temperature for all three sample. This points out that the crystallinity of hematite powder magnifies as the annealing temperature gets risen up. The crystallite size of this sample were calculated by Debye-Sherrer"s equation for highest peak at (104) which is as followed:

$$D = \frac{K\lambda}{\beta cos\theta} \quad (1)$$

Where, D indicates particle size, β being Full Width at Half Maximum (FWHM) while λ and θ denotes the wavelength of X-ray diffraction and Bragg angle respectively [10]. From Table 1, We can see that the increment in crystallite size with higher annealing temperature. This magnification in crystallite size might be due to the monoclinic distortion [1, 6-7].

3.2 Microstructure Analysis

The fraction of SEM photographs of all the three hematite samples annealed at 400^o, 600^o and 800^o C respectively are depicted in Fig. 2. It is clearly evident from the SEM picture that the grains are heterogeneous in shape and randomly dispersed throughout the microstructure and it also indicates the presence of lots of porosity. There are some elongated spherical grains which are clustered together as revealed by the photograph. Augmented annealing temperature leads to the formation in larger grain sized hematite particles and a reduction in void space (porosity) which is in a match with past research work [11]. This might be attributed to the phenomenon that boosting in annealing temperature increases the percent crystallinity of hematite nanoparticles and also creates large no. of crystallites which helps to magnify density of the microstructure [8, 11] shown by the image in Fig. 2. Linear Intercept method was employed to calculate the average grain size of hematite particles and listed in Table 2.

3.3 Optical Property

The optical absorption spectra of hematite samples has been measured for the wavelength range 200-800 nm and depicted in Fig. 3 (a). All three samples showed sharp absorption peak in the UV-region. The absorbance capability of this hematite nanoparticles gets increased with increasing annealing temperature. This higher absorption value indicates that the samples are less transmitted within that region [2].

Kubelka-Munk model and the Tauc linearization for indirect transition could be employed to find out the band gap energy for all three hematite samples as follows,

$$\alpha h\vartheta = A(h\vartheta - E_g)^2 \quad (2)$$

where, α being the absorption coefficient, h is plank's constant, hυ is the photon energy and E_g is the optical band energy. The optical band gap was determined by extrapolating the linear portion of the plot to $\alpha^2 = 0$ in the plot of the square of the absorption coefficient versus photon energy (2, 11). The Tauc plot for indirect transmission for all hematite samples are displayed in Fig. 3 (b)-(d). The calculated band gap for all the samples are shown in Table 2.

It is seen that there is an anomaly in increasing band gap with temperatures. At first the band energy increases for samples annealed at 400^o and 600^o C from 4.9 to 4.95 eV, but for sample annealed at 800^o C the band gap declines to 4.3 eV.

4. Conclusions

In contrast, three hematite samples annealed at 400°, 600° and 800° C were produced using simple sol-gel technique. All three samples retained distorted monoclinic structure which was confirmed by XRD and Rietveld refinement. The crystallite sizes were closer to 50 nm. The SEM analysis

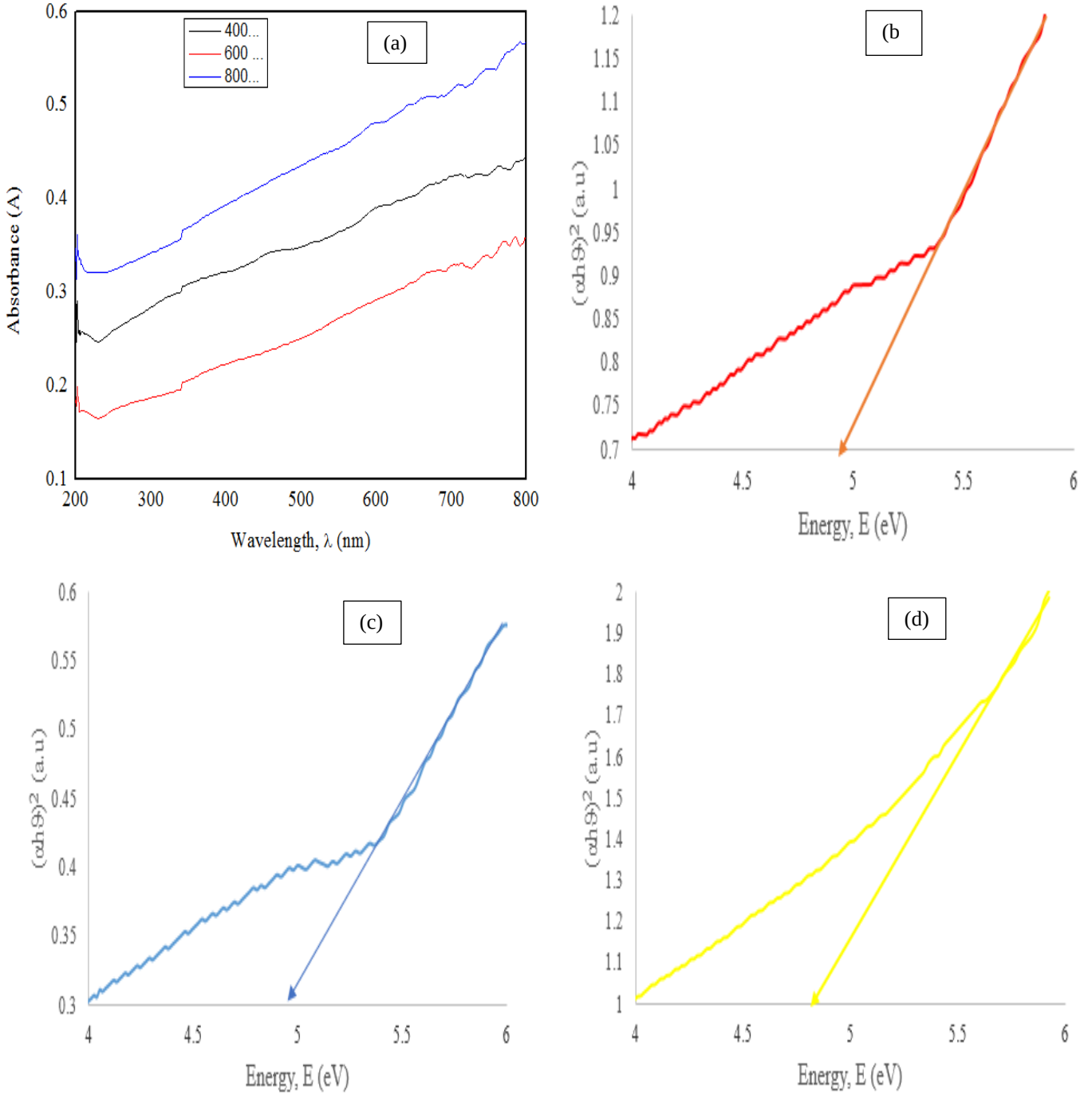

Fig.3: (a) Optical absorption spectra of hematite samples (b) Tauc plot for hematite-400 (c) hematite-600 and (d) hematite-800

exhibitd the presence of elongated abnormal grain within the microstructure. The band gap energy and absorption spectra indicated hematite might be used as insulator in optoelectronic devices.

5. Acknowledgement

Though this research did not get any funding or economic help from the university or agencies or from any company, the corresponding authors are very much grateful to Rajshahi University of Engineering & Technology (RUET) for providing several testing equipments. The special thanks goes to Mr. Humayun Kabir and Tasmia Zaman, Lecturer, Department of GCE, RUET for doing SEM and XRD analysis of hematite samples.

6. References

[1] R. Przenioslo, I. Sosnowska, M. Stekiel, "Monoclinic deformation of the crystal lattice of hematite α-Fe_2O_3", *Physica B*, vol. 4, no. 449, pp. 72-76, 2014.

[2] S. Piccinin, "The band structure and optical absorption of hematite (α-Fe_2O_3): a- first principles GW-BSE study", *Physical Chemistry Chemical Physics*, vol. 1, no. 11, pp. 1-12, 2019.

[3] J. Alexander Morales, "Synthesis of Hematite α-Fe_2O_3 Nano Powders by the controlled precipitation method", *Ciencia en Dessarrolo*, vol. 8, no. 1, pp. 99-107, 2016.

[4] E. A. Campos, D. V. B. S. Pinto, J. I. S. Oliveira, "Synthesis, Characterization and Applications of Iron Oxide Nanoparticles- a Short Review", *J. Aerosp. Technol. Mang*, vol. 7, no. 3, pp. 267-276, 2015.

[5] I. Abdulkadir, A. Babando Aliyu, "Some wet routes for synthesis of hematite nanostructures", *African Journal of Pure and Applied Chemistry*, vol. 7, no. 3, pp. 114-121, 2013.

[6] K. Khan, S. Rehman, H. Ur. Rahman, "Synthesis and application of magnetic nanoparticles", Journal of *Nanomagnetism*, vol. 3, no. 4, pp. 135-159, 2016.

[7] X. Q. Chen, S. B. Wu, R. B. Cao, "Preparation and Characterization of Nanosized Hematite Colloids Using Green Vitriol as Ferrum Source", *Journal of Nanomaterials*, volume 2014, Article ID 749562, 8 pages.

[8] W. Du, S. Yang, F. Pan, "Hydrogen Reduction of Hematite Ore Fines to Magnetite Ores Fines at Low Temperatures", *Journal of Chemistry*, volume 2017, Article ID 1919720, 11 pages.

[9] M. Khalil, J. Yu, N. Liu, "Hydroyhermal synthesis, characterization and growth mechanism of hematite nanoparticles", *J Nanopart Res*, vol. 1, no. 16, pp. 1-10, 2014.

[10] I. N. Kosa, A. Recnik, M. Posfai, "Novel methods for the synthesis of magnetite nanoparticles with special morphologies and textured assemblages*", J Nanopart Res*, vol. 14, no. 11, pp. 1-10, 2012.

[11] S. Bagheri, Chandrappa K. G, S. B. A. Hamid, "Generation of Hematite Nanoparticles via Sol-Gel Method", *Resource Journal of Chemical Sciences*, vol. 3, no. 7, pp. 62-68, 2013.

[12] I. Kazeminezhad, M. Nouri, S. Lakeh, "Synthesis and charaecterization of Iron oxide (Hematite) nanoparticles", J*ournal of Chemistry*, vol. 6, no. 11, pp. 13-15, 2007.

7. Nomenclature

Symbol	Meaning	Unit
θ	Angle of light	degree
d	Grain size	μm
E_g	Band Gap Energy	eV
λ	Wavelength	nm
h	Plank's constant	Dimensionless unit
ϑ	Wavelength of photon	Å